Journal of Materials Chemistry

Cite this: J. Mater. Chem., 2012, 22, 14191

www.rsc.org/materials

PAPER

Light-induced spectral shifting generated from azo-dye doped holographic 2D gratings

Yan Jun Liu,[a] Yu-Chuan Su,[b] Yu-Jui Hsu[b] and Vincent K. S. Hsiao*[b]

Received 22nd February 2012, Accepted 24th May 2012
DOI: 10.1039/c2jm31101a

Optically tunable two-dimensional (2D) gratings were holographically fabricated in azobenzene-doped polymer-dispersed liquid crystals (LCs) using a single diffractive element. Our experiments showed that the diffraction efficiency of the gratings could be switched reversibly upon light irradiation. More importantly, we demonstrated for the first time that the diffractive spectrum from the holographic 2D gratings could be optically tuned by about 24 nm, which might be useful for optically switchable filters and spectroscopic applications. The dynamic switching is attributed to the changes of refractive index modulation between LC-rich and polymer-rich areas due to the *trans–cis*-isomerization-triggered nematic–isotropic phase transition of liquid crystals. In addition, our 2D holographic gratings have polarization-insensitive optical properties for normally incident light. The all-optical tuning behavior is highly reversible and reproducible, making this kind of grating promising in active photonic elements.

Introduction

Light responsive materials are promising candidates for all-optically addressable devices. All-optical control is advantageous since it leverages the benefits of light directed effects—remote, temporal, and spatial control. In the framework of all-optical control, azobenzenes and their derivatives are the most common photoswitchable materials to realize all-optically controllable devices. The reversible *trans–cis* isomerization of azobenzene derivatives by photoirradiation is the root of all-optical control,[1–10] which subsequently results in significant changes of optical properties. Azobenzenes and nematic liquid crystals (LCs) can be mixed together to form a host–guest photo-responsive material system. The photoisomerization of the guest molecules can be used to directly influence the order parameter or isothermally induce the nematic–isotropic phase transition of the host LC system.[11,12]

Holographic polymer-dispersed liquid crystal (H-PDLC)[13] is a well-known photolithographic technique that utilizes a holographic interference patterning onto the LC–prepolymer mixture syrup for fabricating various photonic elements. It offers many advantages including single-step fabrication, unique electro-optical properties, and fast responses. Thus far, many one-, two-, and three-dimensional (1-, 2-, and 3D) photonic structures have been demonstrated using H-PDLC materials.[14–21] LCs exist in a form of droplets of nanoscale size (less than 100 nm) in those holographically fabricated periodic structures. Owing to the high surface-area-to-volume ratio of nanoscale LC droplets, a high electric field (10–20 V μm^{-1}) is often required to drive H-PDLC devices.[22–24] However, the all-organic nature of H-PDLC devices makes them vulnerable to high electric fields and thereby forestalls practical applications. Therefore, alternative approaches to drive the H-PDLC devices are being intensively explored.

In this paper, we report for the first time that the diffractive spectrum from the holographic 2D gratings, fabricated using only a single diffraction element, a photomask, could be optically tuned about 24 nm. By doping a photochromic dye (azobenzene) into the H-PDLC materials, the resulting gratings possess all-optically tunable transmission and diffraction properties. We have characterized their photoresponsive optical properties and analyzed the underlying physical mechanism in details. This all-optical tuning behavior makes this type of grating promising for many active photonic elements, such as optical switches, spatial light modulators, switchable add/drop filters, and spectroscopic applications.

Experimental

The starting prepolymer mixture syrup consisted of 60 wt% monomer, dipentaerythritol penta-/hexa-acrylate (DPHPA), 7 wt% cross-linking monomer, *N*-vinylpyrrolidone (NVP), 1 wt% photoinitiator, rose bengal (RB), and 2 wt% coinitiator, *N*-phenylglycine (NPG), all from Sigma-Aldrich. The photoresponsive material system was a homogeneous mixture of 15 wt% BMAB (4-butyl-4′-methyl-azobenzene) and 85 wt% nematic LC, MDA3461, from Merck (Taiwan Branch). The composition of 30% LC in the LC–prepolymer mixture syrup is the optimized condition in our experiment. The MDA3461 liquid crystal has an

[a]*Institute of Materials Research and Engineering, Agency for Science, Technology and Research (A*STAR), 3 Research Link, Singapore 117602, Singapore*
[b]*Department of Applied Materials and Optoelectronic Engineering, National Chi Nan University, No. 1, University Rd., Puli, NanTou, 54561, Taiwan. E-mail: kshsiao@ncnu.edu.tw*

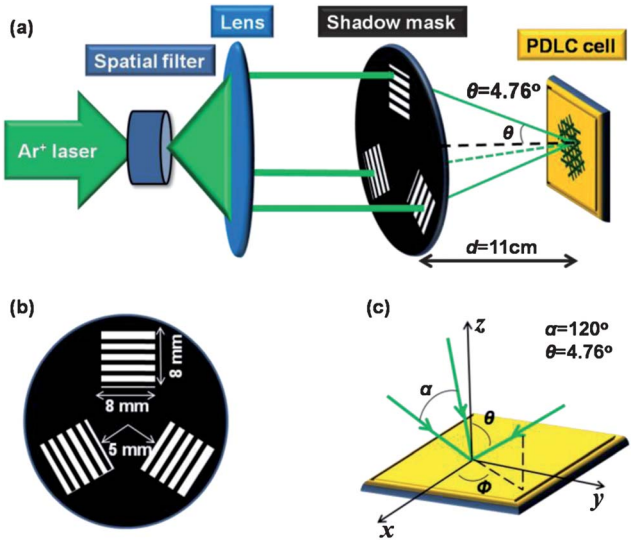

Fig. 1 The schematic of the optical setup (a), specially designed mask (b), and interference configuration of three first-order diffracted beams from the mask (c).

ordinary refractive index (RI) of $n_o = 1.514$ and a birefringence of $\Delta n = 0.258$. Grating sample cells were prepared by placing 15 μL of LC–prepolymer mixture between two glass slides. The thickness of the grating sample was ~3 μm.

The optical setup for the fabrication is schematically illustrated in Fig. 1(a). A photomask was used to create a three-beam interference pattern. The mask consists of three diffraction gratings arranged at 120° relative to one another. In our experiment, each grating on the mask has an area of 8 × 8 mm^2 and the grating period is 6 μm. Fig. 1(b) and (c) show the schematic of the mask and three diffracted beams. This single mask implementation improves the alignment and stability of the optical setup, making it more robust than the multiple beam setups reported previously. An Ar^+ laser operating at 514.5 nm with pumping power ~100 mW cm^{-2} was used to generate the diffraction pattern. When a cell filled with the LC–prepolymer mixture is exposed to the diffraction pattern under pumping power ~10 mW cm^{-2} for 6 min, the LC and polymer will redistribute due to the polymerization of the prepolymer induced by the light, thus forming a 2D structure inside the cell. It is worth mentioning that the light for holographic patterning in our experiment can induce the *cis–trans* isomerization of the BMAB molecules, hence making most BMAB molecules exist in the *trans* state and facilitating the alignment of the LC molecules.

Results and discussion

The electrical field distribution of a multi-beam interferences can generally be described by

$$I(\boldsymbol{r}) = \left[\sum_{j=1}^{n} \boldsymbol{E}_j(\boldsymbol{r})\exp\left(i\boldsymbol{k}\cdot\boldsymbol{r} + i\phi_j\right)\right]\left[\sum_{j=1}^{n} \boldsymbol{E}_j^*(\boldsymbol{r})\exp\left(-i\boldsymbol{k}\cdot\boldsymbol{r} - i\phi_j\right)\right] = \sum_{j=1}^{n}\left|\boldsymbol{E}_j\right|^2 + \sum_{i\neq j}^{n} \boldsymbol{E}_i\cdot\boldsymbol{E}_j^*\exp\left[i\left(\boldsymbol{k}_i - \boldsymbol{k}_j\right)\cdot\boldsymbol{r} + i\phi_{ij}\right] \quad (1)$$

where, $\boldsymbol{E}$ is the amplitude, $\boldsymbol{k}$ is the wave vector, i and j are positive integers, ϕ_{ij} is the initial phase difference between two incident waves, and $\boldsymbol{r}$ is the position vector. As reported before, all 14 Bravais lattices can be fabricated by recording 4 plane wave interference fringes.[25] In our experiment, the beam vectors of the three diffracted first-order beams can be written as

$$\hat{\boldsymbol{k}}_1 = \sin\theta\cos\varphi_1\hat{\boldsymbol{e}}_x + \sin\theta\sin\varphi_1\hat{\boldsymbol{e}}_y + \cos\theta\hat{\boldsymbol{e}}_z \quad (2)$$

$$\hat{\boldsymbol{k}}_2 = \sin\theta\cos\varphi_2\hat{\boldsymbol{e}}_x + \sin\theta\sin\varphi_2\hat{\boldsymbol{e}}_y + \cos\theta\hat{\boldsymbol{e}}_z \quad (3)$$

$$\hat{\boldsymbol{k}}_3 = \sin\theta\cos\varphi_3\hat{\boldsymbol{e}}_x + \sin\theta\sin\varphi_3\hat{\boldsymbol{e}}_y + \cos\theta\hat{\boldsymbol{e}}_z \quad (4)$$

where is a unit wave vector, $\hat{\boldsymbol{e}}$ is a unit coordinate vector, θ is the angle between the diffracted laser beam and the z-axis (the first order diffraction angle), and φ is the angle between the projection of the laser beam on the x–y plane and x-axis [Fig. 1(c)]. Substituting (2)–(4) into (1) with $\theta = 4.76°$, $\varphi_1 = 180°$, $\varphi_2 = -60°$, and $\varphi_3 = 60°$, we have

$$\begin{aligned} I &= (\boldsymbol{E}_1 + \boldsymbol{E}_2 + \boldsymbol{E}_3)\cdot(\boldsymbol{E}_1 + \boldsymbol{E}_2 + \boldsymbol{E}_3)^* \\ &= |\boldsymbol{E}_1|^2 + |\boldsymbol{E}_2|^2 + |\boldsymbol{E}_3|^2 \\ &\quad + 2\boldsymbol{E}_1\cdot\boldsymbol{E}_2\cos\left(-\frac{3}{2}kx\sin\theta + \frac{\sqrt{3}}{2}ky\sin\theta\right) \\ &\quad + 2\boldsymbol{E}_1\cdot\boldsymbol{E}_3\cos\left(-\frac{3}{2}kx\sin\theta - \frac{\sqrt{3}}{2}ky\sin\theta\right) \\ &\quad + 2\boldsymbol{E}_2\cdot\boldsymbol{E}_3\cos\left(\sqrt{3}ky\sin\theta\right) \end{aligned} \quad (5)$$

The simulated 3D interference pattern assuming the same intensity for the three first-order diffracted beams is shown in Fig. 2(a). It is worth mentioning that the period of this triangular lattice equals two thirds of the diffraction grating period, *i.e.*, 4 μm, which does not depend on the wavelength of light.[26]

Fig. 2(b) and (c) are the optical images of a 2D H-PDLC grating observed under a polarized optical microscope (POM) before and after removal of LCs. They reveal a clear hexagonal morphology with a lattice constant of about 3.82 μm, which is in good agreement with the simulation pattern [Fig. 2(a)], considering the general 5–10% volume shrinkage for the acrylate monomer during the photoinduced polymerization.[14] The diffraction patterns of the H-PDLC grating were checked to

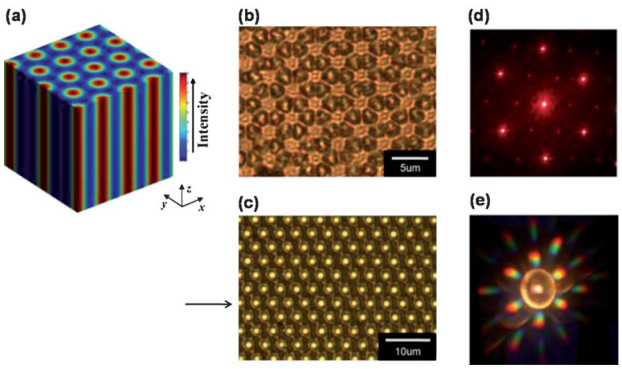

Fig. 2 (a) Simulated 3D interference pattern; observed morphologies of the H-PDLC grating under a POM before (b) and after (c) removal of the LCs; diffraction pattern for a normally incident He–Ne laser beam (d) and a collimated broadband white beam (e).

confirm the quasi-crystal structure. Fig. 2(d) and (e) show the visible diffraction patterns produced by a normally incident He–Ne laser beam operating at 633 nm and by a collimated broad-band white beam, respectively, for our H-PDLC grating sample before the LC removal. The images clearly reveal the presence of quasiperiodicity within the sample. The observed points are sharp and symmetrically distributed. As reported by Gorkhali *et al.*,[27] all diffraction points in the first and higher orders should show an N-fold symmetry and have $2N$ diffracted points, where N is the number of interference beams used to produce the photonic structures. For our case, $N = 3$, in good agreement with the prediction, we can clearly see a 3-fold symmetry and 6 diffracted points for the same order of diffracted beams.

Fig. 3 shows the incident-angle-dependent transmission spectra. At normal incidence, the H-PDLC grating demonstrates a broad trough between 550 nm and 900 nm with the minimum transmission at 660 nm, which arises from the diffraction of the holographic 2D grating. By increasing the incident angle, the trough undergoes a blue shift and becomes broader. In addition, the minimum transmission of the trough reduces, indicating stronger diffraction. The angle dependent dispersion makes our fabricated 2D grating potentially useful for spectroscopic purposes.

Azobenzene-based optical materials have the distinct advantage that they can be optically controlled, which is an important factor for the future development of all-optical devices. Therefore, we investigated the dynamic changes in spectral transmission for the photoresponsive 2D grating structures. In our experiments, a violet laser (405 nm) and a green laser (532 nm)[28] were used to trigger the *trans–cis* and *cis–trans* isomerizations, respectively. Fig. 4 shows the typical dynamic changes in the spectral transmission at normal incidence for a fabricated sample under the violet laser irradiation with different intensities at a fixed irradiating angle of 45° to sample normal. With the increase of the irradiated intensity, the transmission trough blue-shifts by about 24 nm. We also investigated the optically switchable properties of the first-order diffracted light spectrum for the fabricated 2D grating structure (Fig. 5) using a spectrometer (Ocean Optics HR4000). Before light irradiation, the diffracted light shows a lesser amount of red light and that is the reason for the 600–650 nm dip [Fig. 5(a)]. Under light irradiation, the diffracted light intensity within the red regions increases [Fig. 5(b)], due to the enhancement of the diffraction ability of the grating

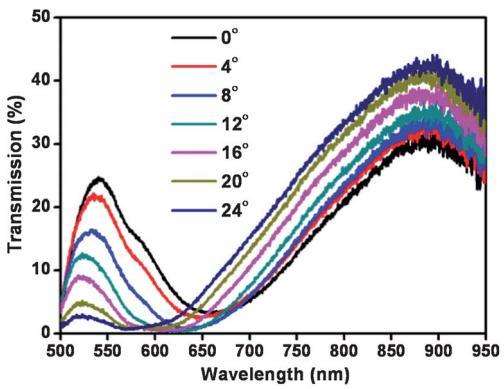

Fig. 3 Angle-dependent transmission spectra for a fabricated 2D grating.

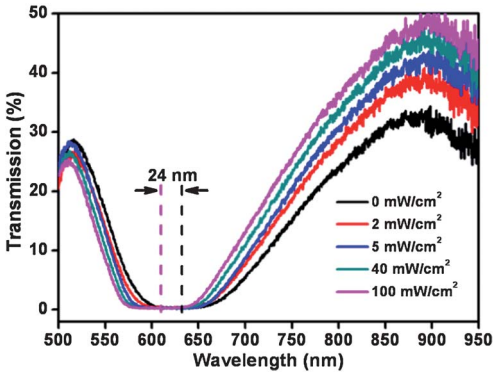

Fig. 4 Dynamic changes of transmission curve at normal incidence for a fabricated sample under various intensities emitting from a 405 nm laser diode.

sample. From Fig. 4 and 5, we conclude that our fabricated 2D grating samples could be used not only as an all-optically tunable filter but also as an all-optically tunable light source for spectrometric purposes.

Fig. 6 shows the time-dependent response of the 2D gratings under alternating laser pumping of two different wavelengths. The switching-on time, which corresponded to the decrease of

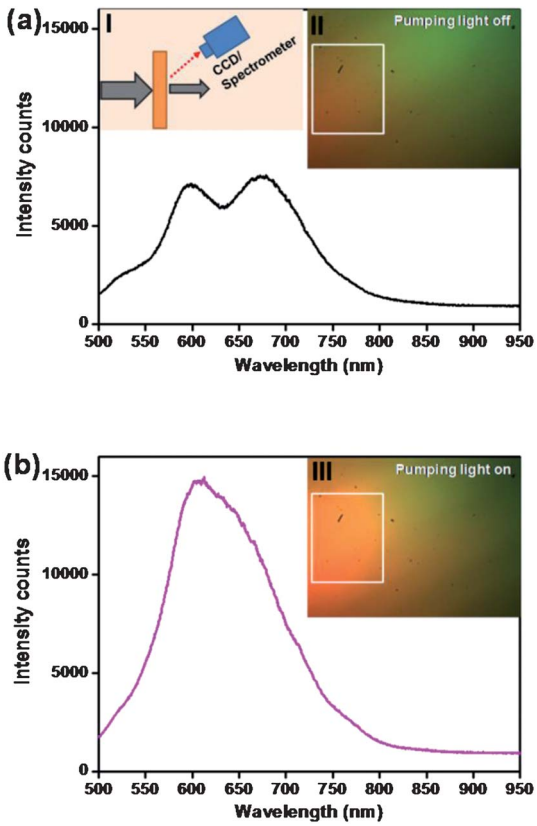

Fig. 5 Comparison of the first-order diffraction spectrum before (a) and after (b) 40 mW cm^{-2} 405 nm laser light irradiation. Inset I shows the schematic setup that uses a CCD or spectrometer to detect the color or spectrum change of the first-order diffraction. Insets II and III show the CCD-captured intensity changes before and after light irradiation (regions indicated by the white lines).

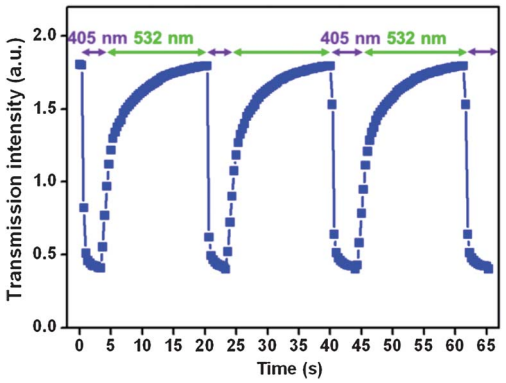

Fig. 6 Photoresponses of the optically tunable H-PDLC gratings under the alternating violet (405 nm) and green (532 nm) laser irradiation. The laser intensity was 40 and 15 mW cm^{-2}, respectively. The processes of violet and green laser irradiation are shown in purple and green, respectively.

diffraction efficiency under 405 nm laser irradiation, was about 4 s, and the switching-off time, which corresponded to the increase of diffraction efficiency under 532 nm laser irradiation, was about 15 s.

The all-optically tunable behavior observed in our experiments could be attributed to the *trans–cis* isomerization-induced nematic–isotropic (N–I) phase change of the LCs. In our H-PDLC grating structures, LC-rich cylindrical arrays are formed and embedded inside the polymer matrices. The cross-linking polymerization of the monomers is accompanied by a contraction of the composites, known as polymerization shrinkage.[14] When the polymeric network shrinks, the LC droplets are compressed, and the rod-shaped LC molecules align along the long symmetric axis of the droplet (a preferential direction). In the case of two-dimensional gratings, liquid crystal cylinders are generally formed. Therefore, LC molecules form homeotropic alignment (*i.e.*, parallel to the polymer wall), as shown in Fig. 7(a). This kind of alignment and polarization insensitivity was also predicted by a previous report.[29] At this alignment state, the probe light, regardless of its polarization, experiences an effective RI, n_{eff}, of the LC region equal to the ordinary RI, n_o, of the LCs, *i.e.*, $n_{eff} = n_o = 1.514$. Only when the RI of polymer is exactly equal to that of LCs at homeotropic alignment can complete darkness of the 2D grating be observed under crossed polarizers. However, in practice, the refractive indices of polymer and LCs are not totally the same. The practical value for the cured polymer is about 1.529,[30] which is slightly different from that of LCs. Such a difference in RI will cause sufficient phase retardation, hence inducing obvious contrast in the brightness, as observed in Fig. 2. Upon the violet photoirradiation, the azo-LC molecules absorb the violet light and then transform from *trans* to *cis*, inducing the N–I phase transition of the LCs, as shown in Fig. 7(b). The empirical effective index for an isotropic LC can be estimated as $n_{iso} \cong (2n_o + n_e)/3$. For the LC MDA3461 used in our experiment, this value is $n_{iso} = 1.60$. At the isotropic state, $n_{eff} = n_{iso} = 1.60$. Note that the RI of polymer is unaltered after violet light irradiation, $n_{poly} = 1.5$. Therefore, the index modulation, Δn, between the LC-rich and polymer-rich regions inside the 2D grating structure increases when the N–I phase transition of the LCs occurs. On the other hand, our 2D gratings can simply be considered as three multiplexed gratings with a 60° intersecting angle. For a grating, the magnitude of the diffraction efficiency strongly depends on the diffraction regime determined by the parameter $Q = 2\pi\lambda L/n_o\Lambda^2$, where λ is the visible wavelength, Λ is the grating period (~4 μm), L is the film thickness (~3 μm), and n_o is the average RI. Here, n_o is estimated to be ~1.55 from the ratio of LC and polymer molecules in the PDLC. The parameter Q is calculated to be <1. As a result, the fabricated grating works in the Raman-Nath regime. The first-order diffraction efficiency is therefore given by $\eta = J_1^2(2\pi\Delta n/\lambda)$ where J_1 is the first-order Bessel function of the first kind. Intuitive calculations from the equation show that the diffraction efficiency for the shorter wavelengths increases exponentially faster

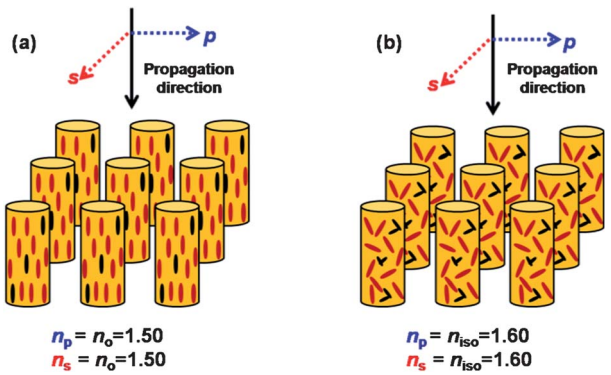

Fig. 7 The proposed model for the alignment of LC molecules inside the cylindrical polymeric cavities before and after light pump.

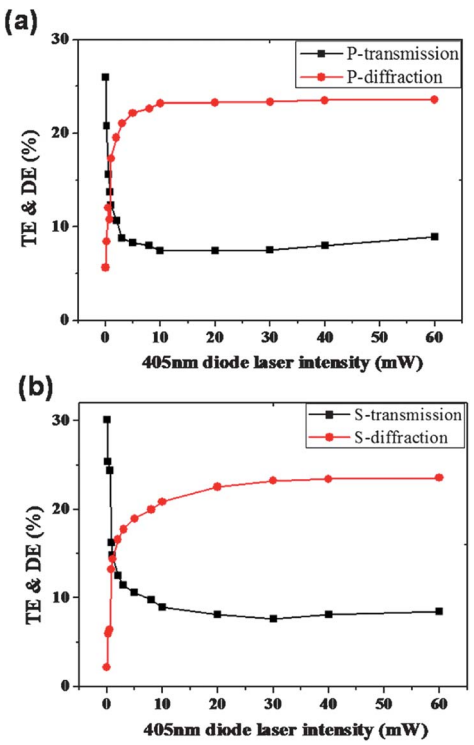

Fig. 8 Changes of transmission and diffraction as a function of irradiated laser intensity for both p- and s-polarized probe light.

than that for the longer wavelengths. As a result, we observed an increase of the diffraction intensity. More importantly, the larger increase in the diffraction efficiency for shorter wavelengths than for longer wavelengths leads to a blue shift as the RI modulation, Δn, increases.

From the above discussion, another distinct advantage of our H-PDLC gratings is that they show polarization-independent optical behavior in both transmission and diffraction at the normal incidence, which is important for many optical devices that require polarization-insensitive operation. As a further confirmation, the polarization-dependent transmission and diffraction were measured as a function of pumping intensity. The results are shown in Fig. 8. From Fig. 8(a) and (b), it can be seen that both p- and s-polarized light show very similar dynamic behavior in both transmission and diffraction. More importantly, there are only slight differences in the TE and DE values for both p- and s-polarized light, which experimentally confirms that our 2D gratings have polarization-insensitive optical properties for normally incident light.

Conclusion

We have demonstrated, for the first time, the light-induced spectral shifting from a 2D grating fabricated by a photolithographic technique that utilizes a holographic interference pattern. This method offers simple, single-step, and low-cost fabrication compared to conventional lithography. Upon light irradiation, the diffraction of the 2D gratings was switched reversibly. The physical mechanism for the switching effect was the *trans–cis*-isomerization-induced N–I phase change of the LCs. Our holographic 2D gratings have also demonstrated polarization-insensitive optical properties for normally incident light. The demonstrated optically tunable 2D diffractive photonic structures are potentially useful for many active photonic elements, such as optical switches, spatial light modulators, switchable add/drop filters, and spectroscopic applications.

Acknowledgements

This work is supported by the National Science Council, Taiwan, under project no. 100-2628-E260-003-MY3 and by the AFOSR/AOARD research grant no. 124023.

Notes and references

1 A. Urbas, J. Klosterman, V. Tondiglia, L. Natarajan, R. Sutherland, O. Tsutsumi, T. Ikeda and T. Bunning, *Adv. Mater.*, 2004, **16**, 1453.
2 S. Huang, S. Wu and A. Y. Fuh, *Appl. Phys. Lett.*, 2006, **88**, 041104.
3 U. A. Hrozhyk, S. V. Serak, N. V. Tabiryan and T. J. Bunning, *Adv. Mater.*, 2007, **19**, 3244–3247.
4 L. De Sio, A. Veltri, C. Umeton, S. Serak and N. Tabiryan, *Appl. Phys. Lett.*, 2008, **93**, 181115.
5 V. K. S. Hsiao and W.-T. Chang, *Appl. Phys. B: Lasers Opt.*, 2010, **100**, 539–546.
6 Y.-C. Su, C.-C. Chu, W.-T. Chang and V. K. S. Hsiao, *Opt. Mater.*, 2011, **34**, 251–255.
7 Y. J. Liu, H. T. Dai and X. W. Sun, *J. Mater. Chem.*, 2011, **21**, 2982–2986.
8 N. Kawatsuki and Emi Uchida, *Appl. Phys. Lett.*, 2003, **83**, 1560–1562.
9 R. A. van Delden, T. Mecca, C. Rosini and B. L. Feringa, *Chem.–Eur. J.*, 2004, **10**, 61–70.
10 M.-H. Wu, C.-C. Chu, M.-C. Cheng and V. K. S. Hsiao, *Mol. Cryst. Liq. Cryst.*, 2012, **557**, 176–189.
11 K. Ichimura, *Chem. Rev.*, 2000, **100**, 1847–1873.
12 Y. J. Liu, Y. B. Zheng, J. Shi, H. Huang, T. R. Walker and T. J. Huang, *Opt. Lett.*, 2009, **34**, 2351–2353.
13 T. J. Bunning, L. V. Natarajan, V. P. Tondiglia and R. L. Sutherland, *Annu. Rev. Mater. Sci.*, 2000, **30**, 83–115.
14 R. L. Sutherland, L. V. Natarajan, V. P. Tondiglia and T. J. Bunning, *Chem. Mater.*, 1993, **5**, 1533–1538.
15 M. J. Escuti, J. Qi and G. P. Crawford, *Appl. Phys. Lett.*, 2003, **83**, 1331–1333.
16 R. L. Sutherland, V. P. Tondiglia, L. V. Natarajan, S. Chandra, D. Tomlin and T. J. Bunning, *Opt. Express*, 2002, **10**, 1074–1082.
17 V. P. Tondiglia, L. V. Natarajan, R. L. Sutherland, D. Tomlin and T. J. Bunning, *Adv. Mater.*, 2002, **14**, 187–191.
18 M. J. Escuti and G. P. Crawford, *Opt. Eng.*, 2004, **43**, 1973–1987.
19 Y. J. Liu and X. W. Sun, *Appl. Phys. Lett.*, 2006, **89**, 171101.
20 Y. J. Liu and X. W. Sun, *Jpn. J. Appl. Phys.*, 2007, **46**, 6634–6638.
21 Y. J. Liu, H. T. Dai, E. S. P. Leong, J. H. Teng and X. W. Sun, *Appl. Phys. B: Lasers Opt.*, 2011, **104**, 659–663.
22 Y.-H. Fan, Y.-H. Lin, H. Ren, S. Gauza and S.-T. Wu, *Appl. Phys. Lett.*, 2004, **84**, 1233–1235.
23 Y. J. Liu, X. W. Sun, H. T. Dai, J. H. Liu and K. S. Xu, *Opt. Mater.*, 2005, **27**, 1451–1455.
24 Y. J. Liu, X. W. Sun, J. H. Liu, H. T. Dai and K. S. Xu, *Appl. Phys. Lett.*, 2005, **86**, 041115.
25 L. Z. Cai, X. L. Yang and Y. R. Wang, *J. Opt. Soc. Am. A*, 2002, **19**, 2238–2244.
26 V. Berger, O. Gauthier-Lafaye and E. Costard, *Electron. Lett.*, 1997, **33**, 425–426.
27 S. P. Gorkhali, J. Qi and G. P. Crawford, *J. Opt. Soc. Am. B*, 2006, **23**, 149–158.
28 A. Urbas, V. Tondiglia, L. Natarajan, R. Sutherland, H. Yu, J.-H. Li and T. Bunning, *J. Am. Chem. Soc.*, 2004, **126**, 13580–13581.
29 P. Kossyrev, M. E. Sousa and G. P. Crawford, *Adv. Funct. Mater.*, 2004, **14**, 1227–1232.
30 Y. J. Liu, B. Zhang, Y. Jia and K. S. Xu, *Opt. Commun.*, 2003, **218**, 27–32.